Archival Report

Biological Psychiatry

Continuous Theta Burst Stimulation Improves Long-Term Outcomes in Alcohol Use Disorder by Modulating a Craving-Related Dynamic Network

Liang-Jie-Cheng Huang, Ning-Ning Zeng, Jing-Nan Zhao, Zhou-Kang Wu, Ying-Ying Li, Tian-Zhen Chen, Lei Guo, Wen-Wen Shen, Hui Zheng, Jian-Zhong Di, Jun Yin, and Min Wang

ABSTRACT

BACKGROUND: Alcohol use disorder (AUD) is a chronic relapsing disorder characterized by craving. While continuous theta burst stimulation (cTBS) shows promise for AUD, its long-term effects on drinking reduction and underlying mechanisms remain unclear. We evaluated the 12-month efficacy of right dorsolateral prefrontal cortex (DLPFC) cTBS for reducing alcohol consumption and identified associated neural and molecular mechanisms.

METHODS: Fifty-five patients with alcohol dependence were randomized to receive 20 sessions of active cTBS targeting the right DLPFC or sham cTBS over 2 weeks. Clinical outcomes were evaluated through 5 follow-up assessments over a 12-month period. A functional magnetic resonance imaging cue-reactivity task was used to investigate craving-related neuroplasticity.

RESULTS: Compared with a sham treatment, active cTBS significantly reduced the risk of returning to baseline or higher drinking over 12 months (hazard ratio = 0.488, 95% CI [0.245–0.971]). At the conclusion of treatment, significant group × time interactions were observed for both the Alcohol Use Disorders Identification Test and subjective craving scores. We identified a craving-related network characterized by hyperconnectivity between frontoparietal and subcortical networks alongside hypoconnectivity between visual and ventral attention systems. Network weight changes correlated with immediate and long-term clinical improvements. Transcriptome association analysis revealed that this network's spatial pattern was linked to genes enriched for synaptic transmission and myelination.

CONCLUSIONS: This study provides evidence for the long-term clinical efficacy of cTBS in reducing drinking among individuals with AUD. The identified multiscale biomarker offers new insights into the hierarchical mechanisms by which cTBS achieves this efficacy, highlighting its potential as a circuit-based therapy for addiction.

https://doi.org/10.1016/j.biopsych.2026.05.004

Alcohol use disorder (AUD) is a chronic relapsing condition and a major global public health challenge. Based on 2020 to 2022 population estimates in the DSM-5, the prevalence of AUD in the United States is more than 10% (1). Despite available interventions, the primary challenge in treating AUD remains the persistently high rate of recurrence. Indeed, even with the pharmacotherapies recommended under current guidelines, a return to heavy drinking occurs in approximately 15% to 95% of patients within 3 to 12 months (2). Given these challenges, reducing alcohol consumption is increasingly recognized as a critical therapeutic target alongside abstinence (3,4). Converging lines of evidence indicate that the principal driver of returning to heavy drinking is craving, a multidimensional state involving intense desire, obsessive thoughts, and heightened attention to cues (5–10). Therefore, developing therapeutic interventions that can effectively and durably reduce craving is crucial for promoting drinking reduction and, as such, is among the primary goals in addiction medicine.

To this end, noninvasive brain stimulation techniques, particularly repetitive transcranial magnetic stimulation (rTMS), have shown promise for directly modulating the dysfunctional neural circuits underlying addiction (11,12). Numerous clinical trials have applied rTMS interventions with the primary goal of reducing craving and alcohol consumption (13–19). However, despite these theoretical advantages, the clinical efficacy of rTMS in treating AUD remains inconsistent across trials (11,20,21). While some randomized controlled trials have reported significant reductions in craving and alcohol consumption (14,18), other well-controlled studies have reported no therapeutic advantage over sham stimulation (16,19). These equivocal findings largely stem from a predominant focus on short-term effects, leaving long-term sustainability uncertain. Furthermore, mixed results suggest an incomplete understanding of the underlying mechanisms that may explain why treatment effects vary and whether observed short-term changes in craving-related circuits translate into durable

ISSN: 0006-3223

drinking reduction. Given the complexity of craving (17,22,23), a hierarchical framework is necessary to bridge different levels of analysis. Therefore, to advance AUD interventions, it is critical to track long-term outcomes while also establishing a multilevel framework—spanning molecular mechanisms to dynamic neural circuits (24)—to delineate the craving-related mechanisms that drive durable clinical efficacy.

While many rTMS interventions have focused on increasing activity within the dorsolateral prefrontal cortex (DLPFC) to enhance executive control (13,25,26), the neurobiology of craving is conceptualized as a critical imbalance between hyperactive reward- and salience-processing circuits and dysregulated executive control networks (11,27–29). Recent large-scale neuroimaging and dynamic network studies have revealed that during alcohol or drug cue exposure, the DLPFC exhibits pathological hyperconnectivity with subcortical reward regions (30,31). Crucially, the strength of this aberrant frontostriatal coupling positively correlates with subjective craving severity (32), suggesting that executive resources are functionally "hijacked" to support drug-seeking behaviors. Given this mechanism, continuous theta burst stimulation (cTBS), an efficient protocol capable of inducing long-term depression–like neuroplasticity (33,34), offers a targeted strategy to disrupt and decouple this pathological engagement. Supporting this approach, recent evidence suggests that cTBS targeting the right DLPFC is clinically effective for depression (35) and, crucially, significantly reduces cue-induced craving in individuals with substance dependence (36). This provides the rationale for the study described here, a randomized, double-blind, sham-controlled trial evaluating the long-term (12-month) effects of cTBS targeting the right DLPFC for the treatment of AUD.

The current study used a hierarchical framework designed to mechanistically link craving-related neuroplasticity with long-term drinking reduction. To this end, our design integrated longitudinal clinical assessments with functional magnetic resonance imaging (fMRI)–based cue-reactivity tasks and transcriptome association analyses. This multimodal approach allowed us to identify modulated craving-related neural signatures and explore their molecular basis. Given that craving is a key determinant of recurrence, a central goal of our framework was to test a set of hierarchical hypotheses. First, at the clinical level, we predicted that DLPFC-cTBS would reduce long-term alcohol consumption and attenuate AUD severity. Second, at the neural circuit level, we hypothesized that this reduction in drinking would be associated with the modulation of specific craving-related dynamic network components. Third, at the molecular level, we postulated that the spatial pattern of this craving network would be linked to an underlying AUD-related gene expression profile.

METHODS AND MATERIALS

Participants

This study was a registered, double-blind, randomized controlled trial (ChiCTR2200065453) approved by the Research Ethics Committee of the Harbin First Specialized Hospital. A total of 55 participants with a current DSM-5 diagnosis of moderate to severe AUD were enrolled at the Harbin First Specialized Hospital after eligibility screening (see the Supplemental Methods for detailed inclusion/exclusion criteria). All participants provided written informed consent. The final sample consisted of an active cTBS group (n = 32) and a sham group (n = 23) (50 male, 5 female; mean age ± SD = 46.800 ± 9.478 years).

Procedure and Design

The study involved assessments at baseline followed by a 2-week intervention period, an immediate postintervention assessment, and a 12-month follow-up period. At baseline and postintervention, participants completed a battery of clinical assessments and performed a cue-reactivity task during an fMRI scan. Following baseline testing, participants were randomized via a computer-generated sequence to receive 20 sessions of either active or sham cTBS targeting the right DLPFC over 2 weeks. The complete procedural details are provided in the Supplemental Methods. The study design and analytical pipeline are shown in Figure 1. Throughout the study, all participants were inpatients and received standard pharmacological care (as detailed in Table S1) alongside routine medical monitoring.

Continuous Theta Burst Protocol

Stimulation was delivered using a figure-of-eight coil (model B9076) connected to a CCY-I TMS instrument (Wuhan Yiruide Medical Co., Ltd.). Prior to stimulation, each participant's resting motor threshold (RMT) was determined over the primary motor cortex. The RMT was defined as the lowest intensity required to elicit a motor evoked potential from the first dorsal interosseous muscle in at least 5 of 10 trials, confirmed visually and with electromyography. The right DLPFC target was localized at the F4 position using a 10–20 EEG-based positioning cap. The cTBS protocol followed a standard procedure of 3-pulse bursts at 50 Hz, repeated every 200 ms (5 Hz) for 40 seconds (totaling 600 pulses) at 100% of the individual's RMT. The intervention followed an accelerated schedule with 2 sessions daily for 10 days over a 2-week period. During stimulation, the coil was held tangentially to the scalp with its handle at a 90° angle to the midsagittal line.

Assessment

The primary clinical outcome was long-term alcohol consumption, which was assessed via standardized telephone follow-ups at 1, 3, 6, 9, and 12 months postintervention. During these calls, trained staff verified identity, obtained recent drinking history, and coded alcohol consumption using a 6-level coding system that categorized current status compared with baseline (i.e., abstinence, reduced use, similar use, worsened use, death, or lost to follow-up). Neural cue reactivity was assessed at baseline and postintervention using an fMRI-based cue-reactivity task. Additionally, the severity of AUD was measured using the Alcohol Use Disorders Identification Test (AUDIT) (37), and subjective craving was quantified using a visual analog scale. Complete details regarding all assessments are available in the Supplemental Methods.

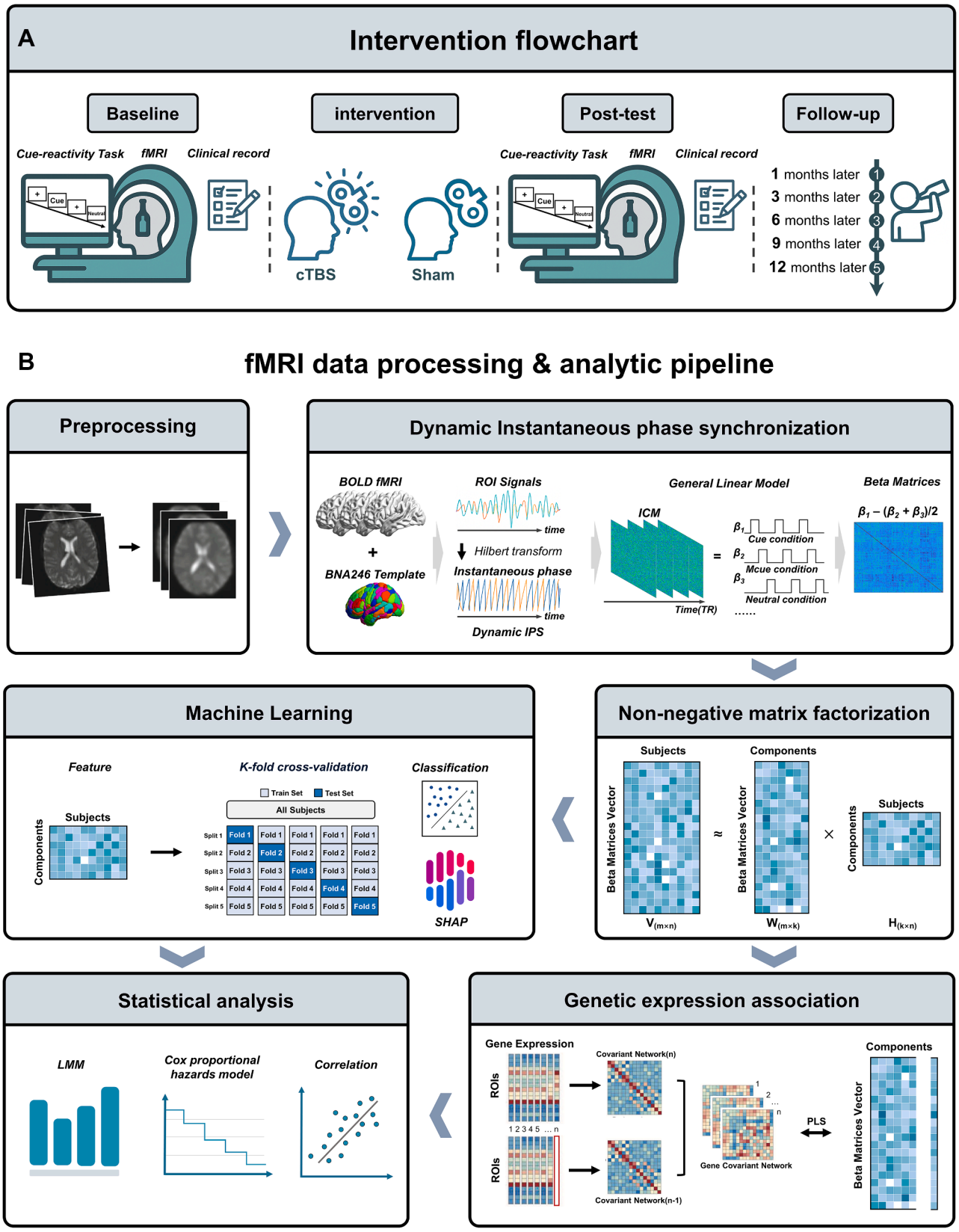
A
Intervention flowchart
Baseline
intervention
Post-test
Follow-up
Cue-reactivity Task
fMRI
Clinical record
cTBS
Sham
Cue-reactivity Task
fMRI
Clinical record
1 months later
3 months later
6 months later
9 months later
12 months later
B
fMRI data processing & analytic pipeline
Preprocessing
Dynamic Instantaneous phase synchronization
BOLD fMRI
BNA246 Template
ROI Signals
time
Hilbert transform
Instantaneous phase
time
Dynamic IPS
General Linear Model
ICM
Time(TR)
Cue condition
Mcue condition
Neutral condition
Beta Matrices
Machine Learning
Feature
Subjects
Components
K-fold cross-validation
Train Set
Test Set
All Subjects
Split 1
Split 2
Split 3
Split 4
Split 5
Fold 1
Fold 2
Fold 3
Fold 4
Fold 5
Classification
SHAP
Non-negative matrix factorization
Subjects
Components
Beta Matrices Vector
Subjects
Components
Beta Matrices Vector
Beta Matrices Vector
Statistical analysis
LMM
Cox proportional hazards model
Correlation
Genetic expression association
Gene Expression
ROIs
Covariant Network(n)
Covariant Network(n-1)
Gene Covariant Network
PLS
Components
Beta Matrices Vector

fMRI Data Collection, Parameters, and Preprocessing

All MRI data were acquired on a 3.0T GE Discovery MR750 scanner. During the fMRI session, participants completed a block-design cue-reactivity task involving the passive viewing of alcohol-related, neutral, and mosaicized control images (three 30-second blocks per condition). Both high-resolution T1-weighted anatomical images and echo-planar images were obtained during each session. Preprocessing was performed using the standard pipeline of DeepPrep (version 25.1.0), a deep learning–based neuroimaging analysis tool (38). The detailed MRI acquisition parameters and the full preprocessing stream are described in Supplemental Methods.

Data Analyses

To analyze task-related brain dynamics, we calculated cue-reactivity functional connectivity using windowless instantaneous phase synchronization to capture dynamic connectivity changes with high temporal resolution (39). The resulting high-dimensional matrices were then decomposed via non-negative matrix factorization (NMF) (40) to identify latent network components. This yielded a basis matrix (W) defining each component's spatial topography and a weight matrix (H) representing its expression per scan. We selected an optimal 30-component solution balancing model stability and reconstruction error. To identify intervention-sensitive components, we applied a machine learning framework with 5-fold cross-validation, using pre-to-post weight difference matrices as features to classify participant intervention labels. After selecting the most accurate classifier, the component with the highest predictive importance was identified using Shapley additive explanations (SHAP) (41). Finally, to explore the molecular basis of this primary predictive component, we used partial least squares (PLS) regression (42) to correlate its spatial topography (W matrix) with Allen Human Brain Atlas gene expression data (43), followed by pathway enrichment analysis. To complement these network-level analyses, we also conducted a standard mass-univariate general linear model (GLM) analysis to examine regional activation changes using a flexible factorial design (group × time) with stringent whole-brain familywise error (FWE) correction ($p < .05$). Complete details of all data analysis steps are provided in the Supplemental Methods.

Statistical Analyses

Statistical analyses were performed in JASP (version 0.95), with significance set at a two-tailed $p < .05$. Baseline demographic and clinical characteristics were compared between groups using independent samples t tests (continuous variables) and χ^2 tests (categorical variables). Long-term outcomes were analyzed using a Cox proportional hazards model to examine the association between treatment group and the risk of returning to baseline or higher levels of drinking. Outcomes were binarized such that maintaining abstinence or reduced use was defined as a favorable outcome (censored), whereas similar use or worsened use constituted an event. Group differences in survival were visualized via Kaplan-Meier curves. To assess the effects of the intervention, linear mixed models (LMMs) were conducted on the AUDIT scores, subjective craving scores, and expression weights of the primary predictive network component. The models included group (active vs. sham), time (preintervention vs. postintervention), and their interaction as fixed effects, with a random intercept for participants.

RESULTS

Behavioral and Clinical Outcomes of the cTBS Intervention

There were no significant demographic or clinical differences between the active and sham groups at baseline (Table 1). In our analysis of long-term outcomes, the Cox proportional hazards model revealed that group was a significant predictor of drinking reduction over the 12-month follow-up period. Specifically, compared with the sham group, the active cTBS group had a significantly lower risk of returning to baseline or higher levels of drinking (hazard ratio [HR] = 0.488, 95% CI [0.245–0.971], $p = .041$). Kaplan-Meier survival analysis further revealed this difference, with a log-rank test confirming significantly different survival curves between the 2 groups ($p = .043$), indicating that the active cTBS group achieved greater reductions in drinking throughout the follow-up period (Figure 2A). A detailed analysis of the changes in alcohol consumption (standard drinks) supporting these findings is provided in the Supplemental Results (Figure S3). In our analysis of immediate clinical outcomes, LMMs revealed statistically significant group × time interactions for both AUDIT scores ($\beta = -1.227$, SE = 0.527, $p = .024$) and subjective craving scores ($\beta = 14.416$, SE = 6.349, $p = .027$). For AUDIT scores, the interaction reflected a decrease in the active group versus an increase in the sham group postintervention, although these within-group changes were not significant (Figure 2B). For subjective craving, simple effects analysis revealed significant reductions in both groups. Detailed results are provided in the Supplemental Results.

Machine Learning Identifies a Treatment-Responsive Network Component (C06)

Prior to network decomposition, a standard whole-brain GLM analysis revealed no suprathreshold clusters for the group ×

Figure 1. An overview of the study design, functional magnetic resonance imaging (fMRI) data processing, and analysis pipeline. **(A)** The experimental procedure, illustrating the 4 main phases: baseline assessment (including clinical records and a cue-reactivity fMRI task), a 2-week intervention period with either active or sham continuous theta burst stimulation (cTBS), an identical postintervention assessment, and a 12-month follow-up. **(B)** Flowchart of the fMRI data processing and analysis pipeline detailing the sequential steps from preprocessing to the final statistical analysis, including dynamic instantaneous phase synchronization, non-negative matrix factorization, machine learning, and gene expression association. ANOVA, analysis of variance; BOLD, blood oxygen level–dependent; ICM, instantaneous coupling matrix; IPS, instantaneous phase synchronization; LMM, linear mixed model; PLS, partial least squares; ROI, region of interest; SHAP, Shapley additive explanations.

Table 1. Demographic Characteristics of the Participants

Characteristics	Active Group, n = 32	Sham Group, n = 23	χ^2/t Value	p Value
Sex				
Female	2	3	0.747	.387[a]
Male	30	20		
Age, Years	45.750 ± 9.685 [30–67]	48.261 ± 9.191 [30–64]	−0.969	.337[b]
Weight, kg	66.813 ± 12.982 [49–100]	63.109 ± 9.427 [50–85]	1.164	.250[b]
Education, Years	9.844 ± 1.648 [9–16]	9.957 ± 1.665 [9–15]	−0.249	.804[b]
AUDIT_pre	31.031 ± 7.046	26.652 ± 11.031	1.796	.078[b]
AUDIT_post	30.500 ± 7.039	27.348 ± 10.560	1.329	.190[b]
Craving_pre[c]	45.625 ± 23.819	55.652 ± 27.605	−1.441	.156[b]
Craving_post[c]	16.563 ± 19.445	12.174 ± 13.803	0.926	.358[b]
CIWA-Ar	24.531 ± 11.924	22.783 ± 10.518	0.563	.576[b]
FTND	4.625 ± 3.045	4.609 ± 3.201	0.019	.985[b]
PSS-10	29.063 ± 9.374	28.304 ± 9.446	0.295	.769[b]
HAMA	12.250 ± 7.002	14.217 ± 6.849	−1.037	.304[b]
HAMD	16.125 ± 10.054	18.348 ± 11.036	−0.776	.441[b]
PSQI	11.031 ± 4.131	9.652 ± 3.433	1.308	.196[b]
HRFS, Habit Subscale	5.026 ± 1.573	4.348 ± 1.892	1.449	.153[b]
HRFS, Reward Subscale	5.380 ± 0.972	5.058 ± 1.181	1.108	.273[b]
HRFS, Fear Subscale	3.943 ± 1.079	3.739 ± 1.055	0.697	.489[b]
Years of Drinking	24.750 ± 10.071	25.913 ± 10.655	−0.412	.682[b]
Alcohol Consumption, Drinks/Calendar Day	22.229 ± 11.127	16.701 ± 15.467	1.543	.129[b]
Duration of Abstinence	6.781 ± 6.332	9.913 ± 7.633	−1.622	.111[b]
Daytime Dysfunction	2.000 ± 0.880	1.696 ± 0.974	1.210	.232[b]
Return to Baseline or Higher Drinking[d]				
1 month later	7 (22.581%)	9 (40.909%)	4.098	.043[e]
3 months later	2 (6.452%)	1 (4.545%)		
6 months later	1 (3.226%)	2 (9.091%)		
9 months later	4 (12.903%)	5 (22.727%)		
12 months later	2 (6.452%)	0 (0%)		
Reduced drinking	15 (48.387%)	5 (22.727%)		

Values are presented as mean ± SD [range], mean ± SD, or n (%).

AUDIT, Alcohol Use Disorders Identification Test; CIWA-Ar, Clinical Institute Withdrawal Assessment for Alcohol, Revised; FTND, Fagerström Test for Nicotine Dependence; HAMA, Hamilton Anxiety Rating Scale; HAMD, Hamilton Depression Rating Scale; HRFS, Habit, Reward, and Fear Scale; PSQI, Pittsburgh Sleep Quality Index; PSS-10, Perceived Stress Scale-10.

[a] p Values were calculated by the χ^2 test.

[b] p Values were calculated by the two-sample t test.

[c] Score from a visual analog scale.

[d] One participant in the active group and one participant in the sham group did not complete the follow-up assessments.

[e] p Values were calculated by the log-rank test (Mantel-Cox test).

time interaction regarding alcohol cue–specific activation under stringent statistical correction (cluster-level FWE $p < .05$) (Figure S5). This absence of gross regional activation changes necessitated a subsequent focus on dynamic network connectivity to capture more subtle circuit-level modulations. To identify intervention-responsive network components, we applied NMF to decompose the dynamic functional connectivity matrices into 30 distinct components. Then we used the components' differential weights to discriminate between the active and sham groups. Among 33 tested algorithms, a cosine K-nearest neighbors classifier achieved the highest prediction accuracy (Figure 3A). Model performance was confirmed by the confusion matrix (Figure 3B) and receiver operating characteristic curve (area under the curve = 0.730) (Figure 3C). We used SHAP to identify the top 5 influential network components, revealing that C06 contributed most to prediction accuracy. The directional relationships predicted by these components for the active and sham groups are shown in Figure 3D and E, respectively. Specifically, the active group was significantly more likely to exhibit a postintervention decrease in the C06 pattern weight.

Network Anatomy of the C06 Component

To characterize the functional architecture of the treatment-responsive C06 component, we summarized the connectivity patterns of its positive and negative networks. Constituent brain regions were mapped to 8 canonical functional networks adapted from Yeo *et al.* (44): the visual network (visual), somatomotor network (SMN), dorsal attention network (DAN), ventral attention network (VAN), limbic network, frontoparietal

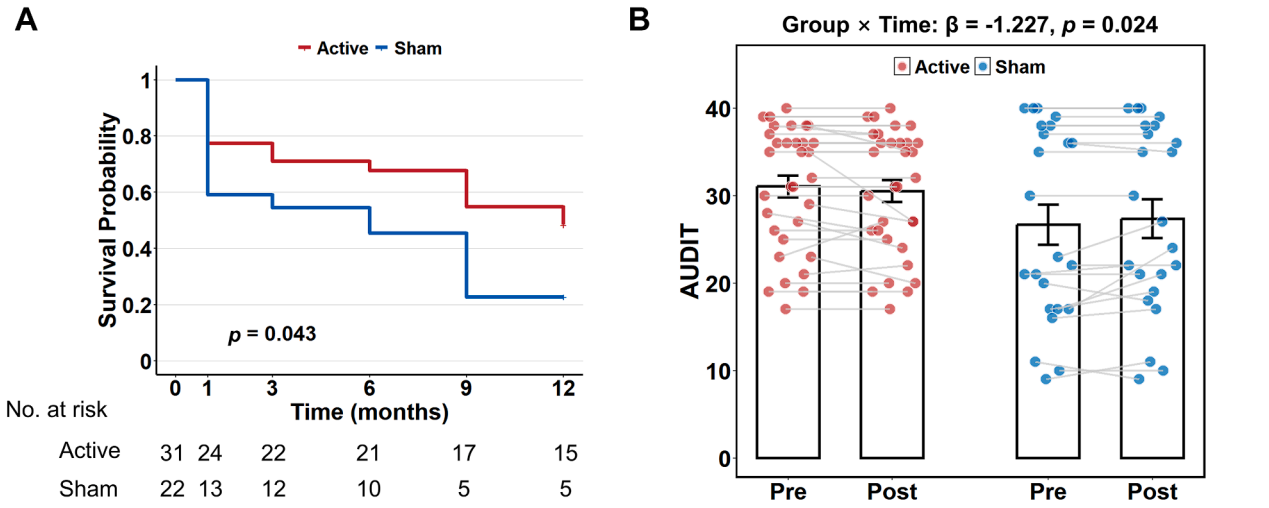

Figure 2. Effects of continuous theta burst stimulation (cTBS) on clinical outcomes. **(A)** Kaplan-Meier survival curves for the 12-month follow-up period. The curves depict the cumulative probability of drinking reduction over time for the active cTBS (red line) and sham cTBS (blue line) groups. The log-rank test revealed a significant difference between the 2 groups, with the active cTBS group showing a higher probability of drinking reduction. **(B)** Bar chart illustrating the group × time interaction effect on Alcohol Use Disorders Identification Test (AUDIT) scores. The data were analyzed using a linear mixed model.

network (FPN), default mode network (DMN), and subcortical network (SCN) (Figure 4A, B). The average connectivity strength within and between these networks is further detailed in Figure 4C, D. The positive C06 network was dominated by connections involving the FPN, which served as a major hub with extensive connections to the SCN, visual network, and

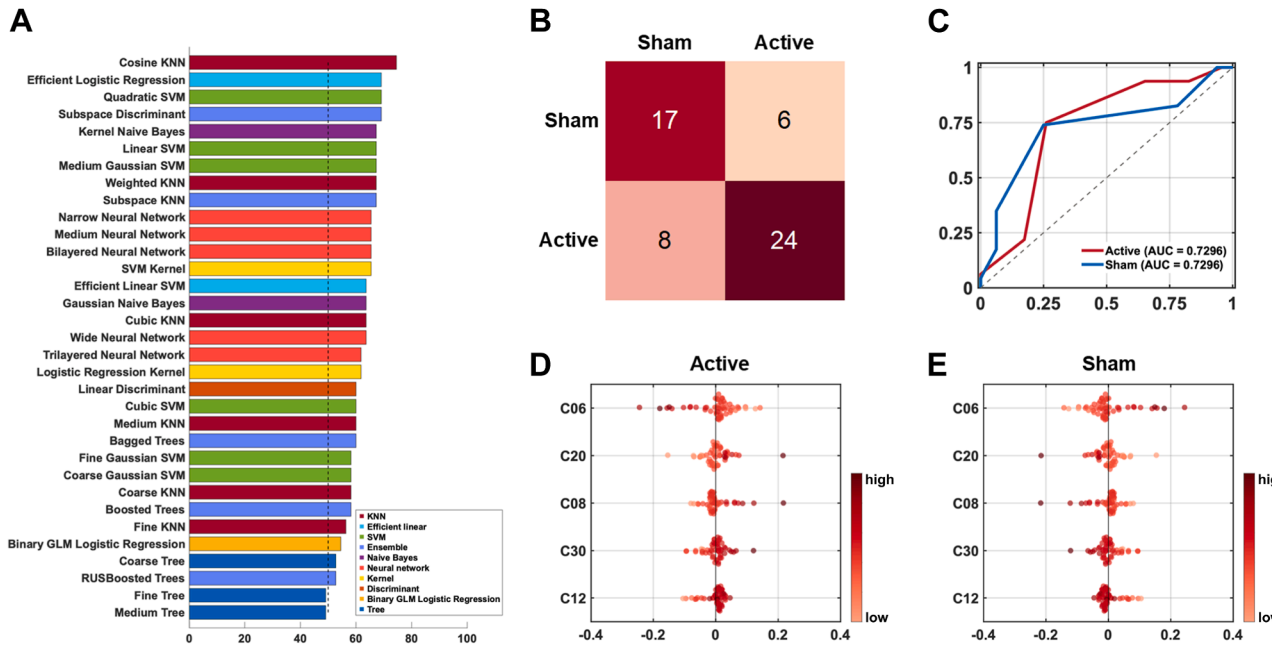

Figure 3. Identification of a treatment-responsive network component using machine learning. **(A)** Prediction accuracy of 33 different classifier models in distinguishing active vs. sham continuous theta burst stimulation (cTBS) groups based on the change in the 30 non-negative matrix factorization (NMF) component weights. The cosine K-nearest neighbors (KNN) model achieved the highest accuracy. **(B)** Confusion matrix for the cosine KNN classifier, showing the number of correctly and incorrectly classified participants in each group. **(C)** Receiver operating characteristic (ROC) curve for the cosine KNN model, with an area under the curve (AUC) of 0.730. **(D, E)** Shapley additive explanations (SHAP) summary plots illustrating the contribution of the top 5 predictive components for each participant in the **(D)** active cTBS group and **(E)** sham cTBS group. The color of each point represents the feature value (deep red indicates high, and light red indicates low). These plots confirm that C06 was the most important feature for the classification. GLM, general linear model; SVM, support vector machine.

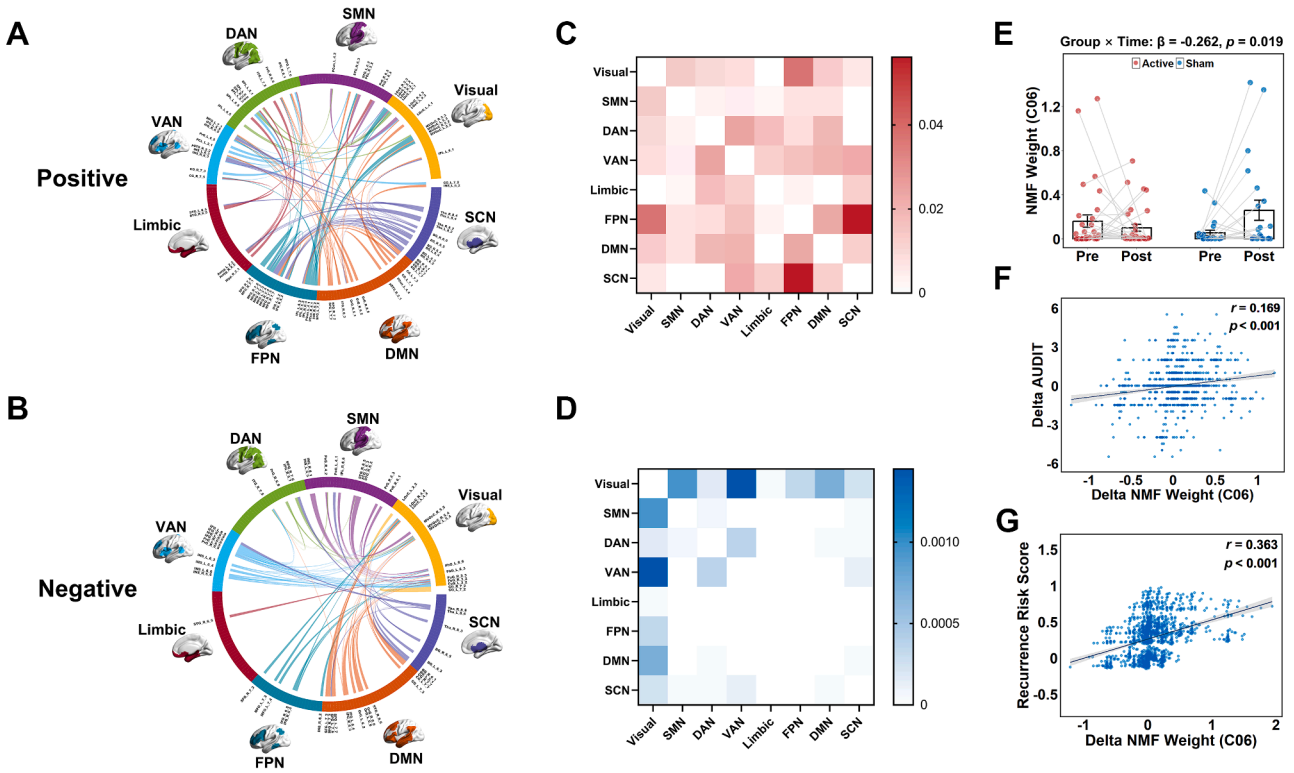

Figure 4. Connectivity patterns and modulation of the C06 component. **(A, B)** Chord diagrams illustrating the top 1% of connections for the **(A)** positive and **(B)** negative edge profiles of the C06 component. Edges are colored according to the 8 functional networks. **(C, D)** Heatmaps depicting the average connectivity strength within and between 8 canonical functional networks for the **(C)** positive and **(D)** negative edge profiles of the C06 component. **(E)** Bar chart illustrating the significant group × time interaction on the C06 component expression weights derived from the linear mixed model. The active continuous theta burst stimulation group showed a decrease in C06 weights postintervention, while the sham group showed an increase. **(F)** Scatter plot depicting the significant positive correlation between the change in C06 component weights (ΔC06) and the change in Alcohol Use Disorders Identification Test (AUDIT) scores (ΔAUDIT), as determined by correlating the intersubject matrices of their pairwise average changes. **(G)** Scatter plot depicting the significant positive correlation between the intersubject similarity matrices of ΔC06 and the individual recurrence risk scores derived from the Cox model, linking neural modulation to long-term drinking reduction. DAN, dorsal attention network; DMN, default mode network; FPN, frontoparietal network; Limbic, limbic network; NMF, non-negative matrix factorization; SCN, subcortical network; SMN, somatomotor network; VAN, ventral attention network; Visual, visual network.

DMN. The DAN also featured prominently, connecting to the VAN, DMN, and limbic network. In contrast, the negative C06 network was dominated by connectivity centered on the visual network, which showed its strongest connections to the VAN, as well as to the SMN, DMN, and FPN. In essence, the positive network of the C06 component reflects the integration of executive control systems with other key brain networks, while its negative network primarily involves connectivity between the sensory and attentional systems.

Modulation of the C06 Component Correlates With Immediate and Long-Term Clinical Outcomes

Having identified C06 as the key treatment-responsive network component, we investigated its direct modulation by the cTBS intervention. For this analysis, one participant from the sham group was excluded as an outlier because the postintervention C06 weight was more than 3 SDs above the group mean. A significant group × time interaction was observed for the C06 component weights derived from the H-matrix ($\beta = -0.262$, SE = 0.108, $p = .019$). This interaction reflected a postintervention decrease in C06 weights for the active group versus an increase for the sham group, although simple effects were not statistically significant (Figure 4E). Notably, the pattern and significance of the interaction effect remained unchanged when the outlier was included (see the Supplemental Results).

To directly link this neural modulation to both immediate and long-term clinical outcomes, we used an approach conceptually inspired by intersubject correlation analysis, which typically assesses the similarity of neural patterns across individuals (45). We constructed intersubject matrices for changes in C06 weights (ΔC06) and AUDIT scores (ΔAUDIT) and for individual recurrence risk scores derived from the Cox model. Each matrix element represented the average change or score for a participant pair. First, the ΔC06 and ΔAUDIT matrices revealed a significant positive correlation ($r = 0.169$, $p < .001$), indicating that participant pairs exhibiting greater C06 weight decreases also showed greater AUDIT score reductions (Figure 4F). Crucially, the ΔC06 matrix also

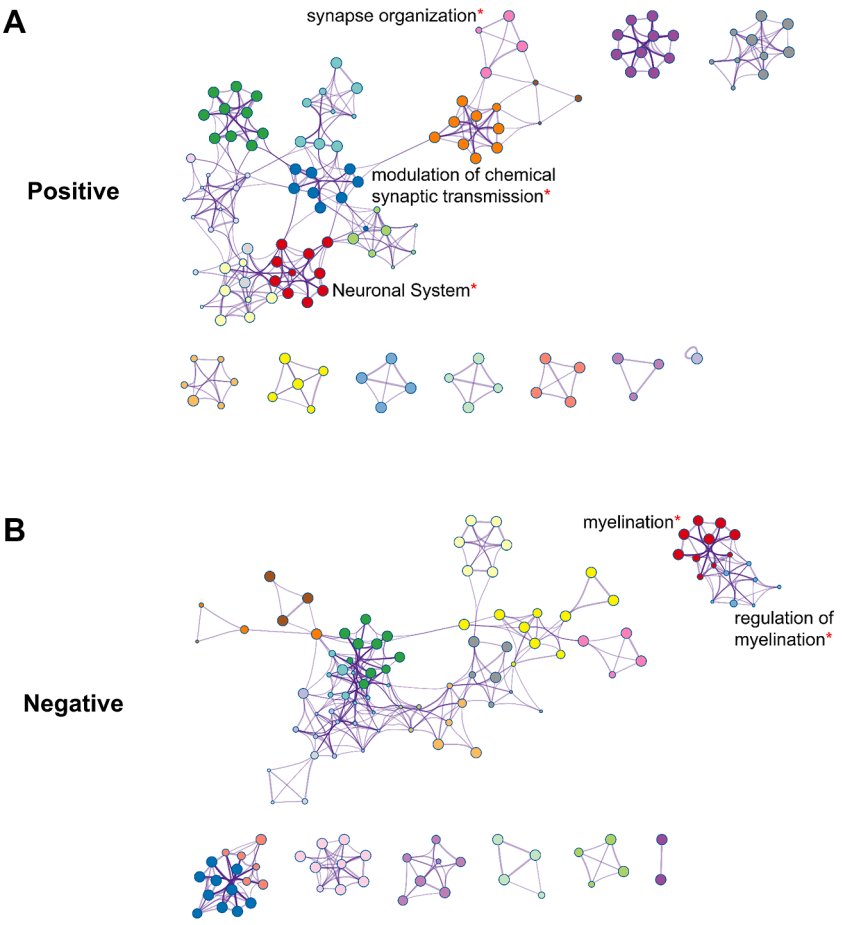

Figure 5. Neuroimaging transcriptomic analysis linking the C06 component to gene expression patterns. **(A, B)** Metascape enrichment analysis networks for the top 1000 partial least squares+ genes associated with the **(A)** positive edge network and **(B)** negative edge network. In the network plots, nodes represent enriched ontology terms, colored by cluster identity. *Indicates the representative enriched ontology term selected by Metascape for each enrichment cluster.

showed a significant positive correlation with the recurrence risk matrix (r = 0.363, $p < .001$), indicating that a greater decrease in C06 component weight was similarly associated with a lower predicted risk of returning to baseline or higher drinking (Figure 4G). Together, these findings demonstrate that the modulation of this network is linked to both immediate clinical improvement and long-term drinking reduction.

Gene Expression Correlates With the C06 Network

To explore the spatial association between gene expression and the C06 network component, we used PLS regression to identify expression patterns correlated with its positive and negative edge connectivity profiles. For both analyses, the first PLS component (PLS1) captured a significant portion of the covariance between gene expression and the network architecture. The PLS1 for the positive edge network explained 12.30% of the variance (p = .027), and its resulting gene expression map was significantly correlated with the C06 positive connectivity pattern (r = 0.163, $p < .001$). Similarly, PLS1 for the negative edge network explained 11.70% of the variance (p = .025), and its expression map was also significantly correlated with the C06 negative connectivity pattern (r = 0.158, $p < .001$).

Next, we performed pathway enrichment analysis on the top-ranking (positively weighted) genes for each network profile. Genes whose expression patterns correlated with the positive edge network were predominantly involved in neuronal processes. The most significant term, “neuronal system” (Reactome Gene Sets), alongside “modulation of chemical synaptic transmission” and “synapse organization” (Gene Ontology [GO] biological processes), underscored a strong association with synaptic function and plasticity (Figure 5A). Conversely, negative edge network genes were enriched primarily in glial cell function, with “myelination” (GO biological processes) as the most significant term. The enrichment of the related term “regulation of myelination” reinforces the finding that this network’s architecture is associated with processes governing neural insulation and signal transmission efficiency (Figure 5B).

DISCUSSION

In this double-blind, randomized controlled trial, we evaluated the long-term effectiveness of cTBS in promoting drinking reduction in individuals with AUD. Our principal clinical finding was that active right DLPFC cTBS reduced the risk of returning to baseline or higher levels of drinking over a 1-year

follow-up compared with sham. To elucidate the underlying mechanisms, we established a hierarchical framework. At the neural circuit level, we identified a specific dynamic network component (C06) that not only served as a biomarker of the cTBS intervention but was also correlated with changes in immediate and long-term clinical symptoms. At the molecular level, we provided exploratory evidence linking this network's spatial topography to genes governing synaptic function and neurodevelopment.

Long-Term and Immediate Clinical Efficacy of cTBS

Our primary clinical findings are consistent with previous studies of rTMS intervention for AUD, which have established the safety and efficacy of multiple high-dose cTBS sessions in treating addiction symptoms (17,18,46). Compared with the economic and time burden of rTMS intervention, intensive accelerated intervention programs, particularly Stanford neuromodulation therapy, have made significant progress in clinical efficacy for depression (47,48). In this study, we considered the application of cTBS in AUD interventions. More importantly, we confirmed the long-term effects of the inhibitory cTBS intervention, which significantly reduced alcohol consumption over the 12-month follow-up period. This finding is particularly significant because the long-term sustainability of TMS-induced gains has been a point of uncertainty in the field, with meta-analyses reporting a scarcity of long-term follow-up data and inconsistent results (22,49). Our study provides empirical evidence for the continued effectiveness of this intervention.

Regarding immediate outcomes, cTBS seemed to exert a protective stabilizing effect. The significant interaction for AUDIT scores highlights the intervention's clinical value; it mitigated the spontaneous deterioration observed in the sham group, preserving stability in active participants. This stabilization, rather than a rapid decline, likely reflects a temporal lag between immediate drinking cessation and the resolution of broader dependence symptoms. Conversely, subjective craving scores decreased significantly in both groups. Consistent with previous addiction trials, this likely reflects a placebo response or the structured inpatient environment (19,50). Such nonspecific improvements highlight the limitations of subjective self-reports and underscore the necessity of our hierarchical framework, which integrates objective neurobiomarkers to capture treatment-specific physiological changes.

Identifying Craving Networks That Respond to Intervention

Using a data-driven approach, we identified a craving-related dynamic network component that was highly responsive to the cTBS intervention. Spatially, this component was defined by 2 distinct profiles, a positive network dominated by hyperconnectivity between the frontoparietal control network and subcortical reward regions and a negative network primarily characterized by visual-centered hypoconnectivity. Crucially, the weight of this network component decreased in the active group after the cTBS intervention and was correlated with the degree of improvement in clinical symptoms. Positive coupling between the FPN and SCN may represent the neural instantiation of the core cognitive conflict in addiction. The FPN mediates top-down executive control, whereas subcortical regions drive bottom-up reward processing (51,52). Meta-analyses have shown that drug-related cues activate frontostriatal circuits (53,54), engaging cognitive functions related to reward, emotion, memory, and decision making (55–57). During cue exposure, the observed hyperconnectivity may suggest that the executive network is "hijacked" or pathologically recruited by the potent salience of drug cues. Therefore, inhibitory cTBS targeting the FPN may disrupt this pathological overcoupling.

In addition, this craving-related network contains an anticorrelation between the visual network and the VAN. The VAN is a critical bottom-up system responsible for reorienting attention toward salient environmental stimuli (58–60). In the context of addiction, highly salient drug cues potently capture attentional resources via this system (61,62). Therefore, the observed hypoconnectivity between the visual network and the VAN during cue exposure may represent a neural signature of attentional conflict. We propose that this decoupling does not reflect an absence of interaction but rather an active, albeit inefficient, attempt by cognitive control systems to suppress the bottom-up attentional capture triggered by the visual processing of alcohol cues (63–65). This interpretation highlights the negative network not as a passive consequence but rather as an active component of the craving state itself. Thus, this anticorrelation may represent the neural substrate for the difficulty in disengaging attention from potent addiction-related stimuli (61,66). Combined with the relevant clinical results, these findings suggest that cTBS seems to improve the pathological connection between cognitive control and reward circuitry by reshaping the topology of craving-related networks, thereby reducing alcohol consumption. Notably, the absence of significant regional activation changes in the standard GLM analysis, contrasted with the robust modulation of network connectivity, reinforces this conceptualization of craving as a network-level phenomenon. This dissociation suggests that the therapeutic efficacy of cTBS is driven by the reorganization of large-scale circuit synchronization rather than by gross alterations in isolated regional excitability.

Transcriptional Correlates of the Treatment-Responsive Network

Our findings further suggest that the distinct connectivity profiles of the treatment-responsive network are supported by transcriptional signatures. The spatial association between the positive edge network and genes pertaining to the neuronal system and synaptic transmission categories is particularly noteworthy. Given that addiction is fundamentally a disorder of maladaptive synaptic plasticity (67,68), these findings provide a molecular basis consistent with the architecture of the network, suggesting that its connectivity pattern may be related to the underlying synaptic machinery. In contrast, the negative edge network was associated with a distinct biological process involving myelination. This enrichment of genes related to glial cell function and neural insulation suggests a novel mechanism. While synaptic plasticity explains

local computational changes, myelination is critical for structural integrity and the efficiency of long-range communication between systems (69,70). This implies that the observed anticorrelation may be related to the underlying white matter architecture. Therefore, a plausible hypothesis is that inhibitory cTBS normalizes network hyperconnectivity by dampening its underlying synaptic machinery, thereby creating a more favorable state for the neuroplastic changes that consolidate long-term recovery.

Limitations

The current findings should be interpreted in the context of several limitations. First, while our sample size was adequate for the observed effects, replication in larger, multicenter trials is necessary to establish generalizability across diverse populations. Second, future research should directly compare our right-sided cTBS regimen with a left-sided intermittent TBS protocol. Third, relying on self-reports without biochemical verification (e.g., ethyl glucuronide) may introduce recall or social desirability biases into the assessment of drinking outcomes. Fourth, participant blinding efficacy might have been suboptimal due to the lack of a dedicated sham coil and was not empirically confirmed via postintervention assessment. Furthermore, the transcriptomic analyses relied on indirect spatial correlations with postmortem atlas data rather than participant-specific measures, precluding causal inference. Finally, future studies could optimize efficacy through personalized approaches, including parameter titration or connectivity-guided targeting.

Conclusions

This trial provides evidence for the long-term clinical efficacy of cTBS for drinking reduction in individuals with AUD. Through a multilevel framework, we identified a dynamic functional connectivity component serving as an objective biomarker of target engagement and therapeutic response. Linking macroscopic network changes to clinical outcomes and underlying molecular substrates offers novel insights into the hierarchical mechanisms of cTBS, highlighting its potential for developing personalized, circuit-based addiction therapies.

ACKNOWLEDGMENTS AND DISCLOSURES

This work has received funding from the Noncommunicable Chronic Diseases–National Science and Technology Major Project (Grant No. 2025ZD0550504 [to J-ZD]), the National Natural Science Foundation of China (Grant No. 82370901 [to J-ZD]), the Shanghai Municipal Science and Technology Commission (Grant No. 24DZ2304800 [to J-ZD]), and the National Natural Science Foundation of China (Grant No. 32371090 [to JY]).

L-J-CH contributed to writing the original draft of the article. L-J-CH, N-NZ, J-NZ, W-WS, JY, and MW contributed to writing, reviewing and editing the article. L-J-CH, N-NZ, J-NZ, Z-KW, T-ZC, LG, W-WS, and MW contributed to methodology. L-J-CH, N-NZ, J-NZ, Y-YL, and MW contributed to investigation. L-J-CH, N-NZ, Z-KW, HZ, J-ZD, and MW contributed to formal analysis. L-J-CH, N-NZ, J-NZ, Y-YL, HZ, and MW contributed to data curation. L-J-CH, N-NZ, J-NZ, HZ, J-ZD, and MW contributed to conceptualization. HZ, J-ZD, and JY contributed to funding acquisition. HZ, J-ZD, JY, and MW contributed to resources.

The authors report no biomedical financial interests or potential conflicts of interest.

Chinese Clinical Trial Registry: Repeated transcranial magnetic stimulation in patients with alcohol addiction; https://www.chictr.org.cn/hvshowproject.html?id=207335&v=1.1; ChiCTR2200065453.

ARTICLE INFORMATION

From the Department of Psychology, Ningbo University, Ningbo, China (L-J-CH, Z-KW, JY, MW); Neuroregulation Center, Wuhu Hospital of Anding Hospital (The Fourth People's Hospital of Wuhu), Wuhu, China (N-NZ, HZ, MW); Cognitive Neuroscience Center, University Medical Center Groningen, Groningen, the Netherlands (N-NZ); Harbin First Specialized Hospital, Harbin, China (J-NZ, Y-YL); Shanghai Mental Health Center, Shanghai Jiao Tong University School of Medicine, Shanghai, China (T-ZC, LG, HZ); Zhejiang Key Laboratory of Drug Addiction and Brain Health, Affiliated Kangning Hospital of Ningbo University, Ningbo, China (W-WS); and Department of Metabolic and Bariatric Surgery, Shanghai Jiao Tong University School of Medicine Affiliated Sixth People's Hospital, Shanghai, China (J-ZD).

L-J-CH, N-NZ, and J-NZ contributed equally to this work.

Address correspondence to Min Wang, Ph.D., at wangmin2@nbu.edu.cn; Jun Yin, Ph.D., at yinjun1@nbu.edu.cn; Jian-Zhong Di, Ph.D., at dijianzhong@sjtu.edu.cn; or Hui Zheng, Ph.D., at zh.dmtr@gmail.com.

Received Nov 6, 2025; revised Apr 30, 2026; accepted May 4, 2026.

Supplementary material cited in this article is available online at https://doi.org/10.1016/j.biopsych.2026.05.004.

REFERENCES

1. Bailey AJ, Quinn PD, McHugh RK (2025): Implications of the shift to DSM-5 for alcohol use disorder prevalence estimates in the National Survey on Drug Use and Health. Addiction 120:184–188.
2. McPheeters M, O'Connor EA, Riley S, Kennedy SM, Voisin C, Kuznacic K, *et al.* (2023): Pharmacotherapy for alcohol use disorder: A systematic review and meta-analysis. JAMA 330:1653–1665.
3. Henssler J, Müller M, Carreira H, Bschor T, Heinz A, Baethge C (2021): Controlled drinking—Non-abstinent versus abstinent treatment goals in alcohol use disorder: A systematic review, meta-analysis and meta-regression. Addiction 116:1973–1987.
4. Sliedrecht W, Roozen H, De Waart R, Dom G, Witkiewitz K (2022): Variety in alcohol use disorder relapse definitions: Should the term "relapse" be abandoned? J Stud Alcohol Drugs 83:248–259.
5. McHugh RK, Fitzmaurice GM, Griffin ML, Anton RF, Weiss RD (2016): Association between a brief alcohol craving measure and drinking in the following week. Addiction 111:1004–1010.
6. Sliedrecht W, de Waart R, Witkiewitz K, Roozen HG (2019): Alcohol use disorder relapse factors: A systematic review. Psychiatry Res 278:97–115.
7. Vafaie N, Kober H (2022): Association of drug cues and craving with drug use and relapse: A systematic review and meta-analysis. JAMA Psychiatry 79:641–650.
8. Bollen Z, Pabst A, Masson N, Wiers RW, Field M, Maurage P (2024): Craving modulates attentional bias towards alcohol in severe alcohol use disorder: An eye-tracking study. Addiction 119:102–112.
9. Miele C, Cabé J, Cabé N, Bertsch I, Brousse G, Pereira B, *et al.* (2023): Measuring craving: A systematic review and mapping of assessment instruments. What about sexual craving? Addiction 118:2277–2314.
10. Wilson SJ (2022): Constructing Craving: Applying the theory of constructed emotion to urge states. Curr Dir Psychol Sci 31:347–354.
11. Mehta DD, Praecht A, Ward HB, Sanches M, Sorkhou M, Tang VM, *et al.* (2024): A systematic review and meta-analysis of neuromodulation therapies for substance use disorders. Neuropsychopharmacology 49:649–680.
12. Sahay S, Rami Reddy MVSR, Lennox C, Wolinsky E, McCullumsmith RE, Singh T (2025): Harnessing neuroimaging-guided transcranial magnetic stimulation for precision therapy in substance use disorders. Mol Psychiatry 30:3804–3816.
13. Belgers M, Van Eijndhoven P, Markus W, Schene A, Schellekens A (2022): rTMS reduces craving and alcohol use in patients with alcohol use disorder: Results of a randomized, sham-controlled clinical trial. J Clin Med 11:951.

14. Harel M, Perini I, Kämpe R, Alyagon U, Shalev H, Besser I, *et al.* (2022): Repetitive transcranial magnetic stimulation in alcohol dependence: A randomized, double-blind, sham-controlled proof-of-concept trial targeting the medial prefrontal and anterior cingulate cortices. Biol Psychiatry 91:1061–1069.
15. Herremans SC, Van Schuerbeek P, De Raedt R, Matthys F, Buyl R, De Mey J, Baeken C (2015): The impact of accelerated right prefrontal high-frequency repetitive transcranial magnetic stimulation (rTMS) on cue-reactivity: An fMRI study on craving in recently detoxified alcohol-dependent patients. PLoS One 10:e0136182.
16. Hoven M, Schluter RS, Schellekens AF, van Holst RJ, Goudriaan AE (2023): Effects of 10 add-on HF-rTMS treatment sessions on alcohol use and craving among detoxified inpatients with alcohol use disorder: A randomized sham-controlled clinical trial. Addiction 118:71–85.
17. Kearney-Ramos TE, Dowdle LT, Lench DH, Mithoefer OJ, Devries WH, George MS, *et al.* (2018): Transdiagnostic effects of ventromedial prefrontal cortex transcranial magnetic stimulation on cue reactivity. Biol Psychiatry Cogn Neurosci Neuroimaging 3:599–609.
18. McCalley DM, Kaur N, Wolf JP, Contreras IE, Book SW, Smith JP, Hanlon CA (2023): Medial prefrontal cortex theta burst stimulation improves treatment outcomes in alcohol use disorder: A double-blind, sham-controlled neuroimaging study. Biol Psychiatry Glob Open Sci 3:301–310.
19. Perini I, Kämpe R, Arlestig T, Karlsson H, Löfberg A, Pietrzak M, *et al.* (2020): Repetitive transcranial magnetic stimulation targeting the insular cortex for reduction of heavy drinking in treatment-seeking alcohol-dependent subjects: A randomized controlled trial. Neuropsychopharmacology 45:842–850.
20. Sorkhou M, Stogios N, Sayrafizadeh N, Hahn MK, Agarwal SM, George TP (2022): Non-invasive neuromodulation of dorsolateral prefrontal cortex to reduce craving in alcohol use disorder: A meta-analysis. Drug Alcohol Depend Rep 4:100076.
21. Treiber M, Tsapakis EM, Fountoulakis K (2025): Repetitive transcranial magnetic stimulation for alcohol craving in alcohol use disorders: A meta-analysis. J Addict Med 19:195–201.
22. Jansen JM, Daams JG, Koeter MWJ, Veltman DJ, van den Brink W, Goudriaan AE (2013): Effects of non-invasive neurostimulation on craving: A meta-analysis. Neurosci Biobehav Rev 37:2472–2480.
23. Perkins KA (2009): Does smoking cue-induced craving tell us anything important about nicotine dependence? Addiction 104:1610–1616.
24. Lee K, Ji JL, Helmer M, Murray JD, Krystal JH, Anticevic A (2026): A framework for advancing mechanistic neuro-behavioral biomarkers in psychiatry. Biol Psychiatry 99:896–908.
25. Herremans SC, Vanderhasselt MA, De Raedt R, Baeken C (2013): Reduced intra-individual reaction time variability during a go–NoGo task in detoxified alcohol-dependent patients after one right-sided dorsolateral prefrontal HF-rTMS session. Alcohol Alcohol 48:552–557.
26. Liu Q, Cui H, Li J, Shen Y, Zhang L, Zheng H (2024): Modulation of dlPFC function and decision-making capacity by repetitive transcranial magnetic stimulation in methamphetamine use disorder. Transl Psychiatry 14:280.
27. Ekhtiari H, Sangchooli A, Carmichael O, Moeller FG, O'Donnell P, Oquendo MA, *et al.* (2024): Neuroimaging biomarkers of addiction. Nat Mental Health 2:1498–1517.
28. Koob GF, Volkow ND (2016): Neurobiology of addiction: A neurocircuitry analysis. Lancet Psychiatry 3:760–773.
29. Zheng H, Zhai T, Lin X, Dong G, Yang Y, Yuan T-F (2024): The resting-state brain activity signatures for addictive disorders. Med 5:201–223.e6.
30. Arias AJ, Ma L, Bjork JM, Hammond CJ, Zhou Y, Snyder A, Moeller FG (2021): Altered effective connectivity of the reward network during an incentive-processing task in adults with alcohol use disorder. Alcoholism Clin & Exp Res 45:1563–1577.
31. Zhang X, Zhang H, Shao Y, Li Y, Zhang F, Zhang H (2025): Common neural patterns of substance use disorder: A seed-based resting-state functional connectivity meta-analysis. Transl Psychiatry 15:190.
32. Ray S, Haney M, Hanson C, Biswal B, Hanson SJ (2015): Modeling causal relationship between brain regions within the drug-cue processing network in chronic cocaine smokers. Neuropsychopharmacology 40:2960–2968.
33. Cole EJ, O'Sullivan SJ, Tik M, Williams NR (2024): Accelerated theta burst stimulation: Safety, efficacy, and future advancements. Biol Psychiatry 95:523–535.
34. Kishi T, Ikuta T, Sakuma K, Hatano M, Matsuda Y, Wilkening J, *et al.* (2024): Theta burst stimulation for depression: A systematic review and network and pairwise meta-analysis. Mol Psychiatry 29:3893–3899.
35. Zhao H, Jiang C, Zhao M, Ye Y, Yu L, Li Y, *et al.* (2024): Comparisons of accelerated continuous and intermittent theta burst stimulation for treatment-resistant depression and suicidal ideation. Biol Psychiatry 96:26–33.
36. Zhao D, Li Y, Liu T, Voon V, Yuan T-F (2020): Twice-daily theta burst stimulation of the dorsolateral prefrontal cortex reduces methamphetamine craving: A pilot study. Front Neurosci 14:208.
37. Babor TF, Higgins-Biddle JC, Saunders JB, Monteiro MG (2001): The Alcohol Use Disorders Identification Test: Guidelines for Use in Primary Care. Geneva: World Health Organization.
38. Ren J, An N, Lin C, Zhang Y, Sun Z, Zhang W, *et al.* (2025): DeepPrep: An accelerated, scalable and robust pipeline for neuroimaging preprocessing empowered by deep learning. Nat Methods 22:473–476.
39. Sheng D, Pu W, Linli Z, Tian GL, Guo S, Fei Y (2023): Aberrant global and local dynamic properties in schizophrenia with instantaneous phase method based on Hilbert transform. Psychol Med 53:2125–2135.
40. Lee DD, Seung HS (1999): Learning the parts of objects by non-negative matrix factorization. Nature 401:788–791.
41. Lundberg SM, Lee SI (2017): A unified approach to interpreting model predictions. Adv Neural Inf Process Syst 30:4765–4774.
42. McIntosh AR, Mišić B (2013): Multivariate statistical analyses for neuroimaging data. Annu Rev Psychol 64:499–525.
43. Hawrylycz MJ, Lein ES, Guillozet-Bongaarts AL, Shen EH, Ng L, Miller JA, *et al.* (2012): An anatomically comprehensive atlas of the adult human brain transcriptome. Nature 489:391–399.
44. Yeo BTT, Krienen FM, Sepulcre J, Sabuncu MR, Lashkari D, Hollinshead M, *et al.* (2011): The organization of the human cerebral cortex estimated by intrinsic functional connectivity. J Neurophysiol 106:1125–1165.
45. Chen G, Shin YW, Taylor PA, Glen DR, Reynolds RC, Israel RB, Cox RW (2016): Untangling the relatedness among correlations, part I: Nonparametric approaches to inter-subject correlation analysis at the group level. Neuroimage 142:248–259.
46. Hanlon CA, Dowdle LT, Correia B, Mithoefer O, Kearney-Ramos T, Lench D, *et al.* (2017): Left frontal pole theta burst stimulation decreases orbitofrontal and insula activity in cocaine users and alcohol users. Drug Alcohol Depend 178:310–317.
47. Cole EJ, Stimpson KH, Bentzley BS, Gulser M, Cherian K, Tischler C, *et al.* (2020): Stanford accelerated intelligent neuromodulation therapy for treatment-resistant depression. Am J Psychiatry 177:716–726.
48. Cole EJ, Phillips AL, Bentzley BS, Stimpson KH, Nejad R, Barmak F, *et al.* (2022): Stanford neuromodulation therapy (SNT): A double-blind randomized controlled trial. Am J Psychiatry 179:132–141.
49. Kim DJ, Jeong H, Kim SY, Kim YH, Yim HW (2025): Efficacy of non-invasive brain stimulation in reducing craving in patients with alcohol use disorder: Systematic review and meta-analysis. BMC Psychiatry 25:496.
50. Del Re AC, Maisel N, Blodgett JC, Wilbourne P, Finney JW (2013): Placebo group improvement in trials of pharmacotherapies for alcohol use disorders: A multivariate meta-analysis examining change over time. J Clin Psychopharmacol 33:649–657.
51. Bechara A (2005): Decision making, impulse control and loss of willpower to resist drugs: A neurocognitive perspective. Nat Neurosci 8:1458–1463.
52. Volkow ND, Michaelides M, Baler R (2019): The neuroscience of drug reward and addiction. Physiol Rev 99:2115–2140.
53. Engelmann JM, Versace F, Robinson JD, Minnix JA, Lam CY, Cui Y, *et al.* (2012): Neural substrates of smoking cue reactivity: A meta-analysis of fMRI studies. Neuroimage 60:252–262.
54. Hill-Bowen LD, Riedel MC, Poudel R, Salo T, Flannery JS, Camilleri JA, *et al.* (2021): The cue-reactivity paradigm: An ensemble of networks driving attention and cognition when viewing drug and natural reward-related stimuli. Neurosci Biobehav Rev 130:201–213.

55. Ma N, Liu Y, Li N, Wang C-X, Zhang H, Jiang X-F, *et al.* (2010): Addiction related alteration in resting-state brain connectivity. Neuroimage 49:738–744.
56. Rodríguez GC, Russell MA, Claus ED (2025): Systematic review on resting-state fMRI in people with AUD and people who binge drink. Mol Psychiatry 30:752–762.
57. Shokri-Kojori E, Tomasi D, Wiers CE, Wang GJ, Volkow ND (2017): Alcohol affects brain functional connectivity and its coupling with behavior: Greater effects in male heavy drinkers. Mol Psychiatry 22:1185–1195.
58. Corbetta M, Shulman GL (2002): Control of goal-directed and stimulus-driven attention in the brain. Nat Rev Neurosci 3:201–215.
59. Corbetta M, Patel G, Shulman GL (2008): The reorienting system of the human brain: From environment to theory of mind. Neuron 58:306–324.
60. Vossel S, Geng JJ, Fink GR (2014): Dorsal and ventral attention systems: Distinct neural circuits but collaborative roles. Neuroscientist 20:150–159.
61. Kilts CD, Kennedy A, Elton AL, Tripathi SP, Young J, Cisler JM, James GA (2014): Individual differences in attentional bias associated with cocaine dependence are related to varying engagement of neural processing networks. Neuropsychopharmacology 39:1135–1147.
62. Janes AC, Farmer S, Peechatka AL, Frederick BDB, Lukas SE (2015): Insula–dorsal anterior cingulate cortex coupling is associated with enhanced brain reactivity to smoking cues. Neuropsychopharmacology 40:1561–1568.
63. Goldstein RZ, Volkow ND (2011): Dysfunction of the prefrontal cortex in addiction: Neuroimaging findings and clinical implications. Nat Rev Neurosci 12:652–669.
64. Hanlon CA, Dowdle LT, Naselaris T, Canterberry M, Cortese BM (2014): Visual cortex activation to drug cues: A meta-analysis of functional neuroimaging papers in addiction and substance abuse literature. Drug Alcohol Depend 143:206–212.
65. Strosche A, Zhang X, Kirsch M, Hermann D, Ende G, Kiefer F, Vollstädt-Klein S (2021): Investigation of brain functional connectivity to assess cognitive control over cue-processing in Alcohol Use Disorder. Addict Biol 26:e12863.
66. Hester R, Garavan H (2009): Neural mechanisms underlying drug-related cue distraction in active cocaine users. Pharmacol Biochem Behav 93:270–277.
67. Hyman SE, Malenka RC, Nestler EJ (2006): Neural mechanisms of addiction: The role of reward-related learning and memory. Annu Rev Neurosci 29:565–598.
68. Kauer JA, Malenka RC (2007): Synaptic plasticity and addiction. Nat Rev Neurosci 8:844–858.
69. Dutta DJ, Woo DH, Lee PR, Pajevic S, Bukalo O, Huffman WC, *et al.* (2018): Regulation of myelin structure and conduction velocity by perinodal astrocytes. Proc Natl Acad Sci U S A 115:11832–11837.
70. Fields RD (2015): A new mechanism of nervous system plasticity: Activity-dependent myelination. Nat Rev Neurosci 16:756–767.